Rapid Assembly and Collective Behavior of Microtubule Bundles in the Presence of Polyamines

Loïc Hamon,* Philippe Savarin, Patrick A. Curmi, and David Pastré*
Laboratoire Structure-Activité des Biomolécules Normales et Pathologiques, Institut National de la Santé et de la Recherche Médicale, U829, and Université Evry-Val d'Essonne, EA3637, Evry, France

ABSTRACT Microtubules (MTs) are cylindrical cytoskeleton polymers composed of α-β tubulin heterodimers whose dynamic properties are essential to fulfill their numerous cellular functions. In response to spatial confinement, dynamic MTs, even in the absence of protein partners, were shown to self-organize into higher order structures (spindle or striped structures) which lead to interesting dynamical properties (MT oscillations). In this study, we considered the assembly and sensitivity of dynamic MTs when in bundles. To perform this study, spermine, a natural tetravalent polyamine present at high concentrations in all eukaryote cells, was used to trigger MT bundling while preserving MT dynamics. Interestingly, we first show that, near physiological ionic strengths, spermine promotes the bundling of MTs whereas it does not lead to aggregation of free tubulin, which would have been detrimental to MT polymerization. Experimental and theoretical results also indicate that, to obtain a high rate of bundle assembly, bundling should take place at the beginning of assembly when rapid rotational movements of short and newly nucleated MTs are still possible. On the other hand, the bundling process is significantly slowed down for long MTs. Finally, we found that short MT bundles exhibit a higher sensitivity to cold exposure than do isolated MTs. To account for this phenomenon, we suggest that a collective behavior takes place within MT bundles because an MT entering into a phase of shortening could increase the probability of the other MTs in the same bundle to enter into shortening phase due to their close proximity. We then elaborate on some putative applications of our findings to in vivo conditions including neurons.

INTRODUCTION

Microtubules (MTs) are cylindrical hollow polymers made of tubulin heterodimers that are essential in eukaryotic cells for organizing the cytoplasm, polarity establishment, morphogenesis, and cell division. MTs display surprisingly complex behaviors both in terms of dynamical properties and spatial organization. The formation of the mitotic spindle, a MT superstructure endowing cell division, is a well-known example. Its formation requires the action of multiple MT protein partners (MAPs) and molecular motors (1). At first sight, we may then suppose MT complexity to mostly rely on the presence of numerous protein partners. However, even in their absence, MTs can display surprising self-organizing properties in vitro such as the formation of MT spindles in micro devices (2,3) or striped structures in spectrophotometer cells (4,5). Interestingly, higher order organization of MTs is generally correlated with unexpected dynamical properties. A well-known example is that of MT oscillations, when striped MT structures collectively alternate between growing and shortening phases (6). Spatial ordering of MTs relies on weak and dynamic interactions among tubulin dimers and, consequently, both the spatial organization and kinetics of MTs are sensitive to external perturbations like spatial confinement (7), and weak forces generated by gravity and magnetic fields (8–10).

In this study, we explore what happens if we introduce a weak self-attraction force between tubulin dimers. Such a force is generally associated with MT bundling and stabilization. However, while MT bundling mediated by stabilizing agents like tau (11,12) and MAP2 (13) has been thoroughly investigated and indeed leads to the formation of stable MT bundles, little is known about the dynamical properties of bundles made of dynamic MTs (14). To tackle this issue, we chose a cationic polyamine, spermine (Spm), to both trigger a weak electrostatic attraction force between highly anionic tubulin dimers (15) and preserve MT dynamics. Interestingly, Spm is a natural polyamine present at millimolar concentrations in all eukaryotic organisms (16) and therefore a putative counterion of MTs in vivo (15).

The key finding of this work is that, starting from free tubulin and Spm, MTs can be assembled into short micrometric bundles in less than half a minute, whereas, when bundles are to be formed by adding Spm to preformed MTs, bundling occurs at rates orders-of-magnitude lower. Our scaling arguments suggest that MT rotational diffusion, which decreases with MT length, is rate-limiting in the bundling process. This is why bundling occurs at its highest rate for short, newly nucleated MTs and the bundling process then stops when MT length reaches a critical value above which diffusion is hindered.

We also show that MT bundles formed by Spm display a higher sensitivity to brief cold exposure compared to isolated MTs. Such sensitivity results from a collective behavior within MT bundles in the sense that one MT destabilization event in a given bundle may raise the probability of other MTs in the bundle to undergo catastrophe. This was previously noted for MTs growing from axonemes (14).

Submitted November 17, 2010, and accepted for publication May 10, 2011.

*Correspondence: david.pastre@univ-evry.fr or loic.hamon@univ-evry.fr

Editor: Lewis H. Romer.

0006-3495/11/07/0205/12 $2.00

doi: 10.1016/j.bpj.2011.05.022

Interestingly, in contrast with MT oscillations (6), which occur high above normal tubulin concentrations (>80 μM), the collective response of MTs within bundles arises whatever the concentration of tubulin dimers (here from 16 μM to 40 μM) and thus possibly under physiological conditions (~20 μM tubulin). We then evaluate, using scaling arguments, whether a collective behavior of MTs in bundles occurs and which parameters facilitate its arousal. Finally, we discuss the possible occurrence of dynamic MT bundles in vivo and whether the concepts regarding rapid assembly and high sensitivity of MT bundles can be applied to specific functions such as neurite outgrowth or growth cone turning.

METHODS

Tubulin preparation

Tubulin was purified from sheep brain crude extracts as described previously (17). Aliquots were stored at −80°C in 50 mM MES-KOH pH 6.8, 0.5 mM dithiothreitol, 0.5 mM EGTA, 0.25 mM $MgCl_2$, 0.5 mM EDTA, 0.1 mM GTP, 30% glycerol (v/v). Before use, an additional cycle of polymerization was performed in 50 mM MES-KOH pH 6.8, 0.5 mM EGTA, 4 mM $MgCl_2$, 0.5 mM EDTA, 0.6 mM GTP, 30% glycerol. MTs were then sedimented by centrifugation (52,000 × g, 30 min at 37°C) and the MT pellet was resuspended in 25 mM MES-KOH pH 6.8, 0.5 mM EGTA, 1 mM DTT and disassembled at 4°C for 20 min. To remove tubulin aggregates, another ultracentrifugation (52,000 × g, 20 min) was performed at 4°C.

Preparation of CPAP fragment

PN2-3 region of CPAP (amino acids 311–422) was expressed according to the protocol described by Cormier et al. (34). Shortly, this domain was expressed in the BL21 (DE3) *E. coli* strain. Three hours after induction, bacteria were pelleted, sonicated, and then centrifuged. Supernatant was boiled and then centrifuged. PN2-3 pure fractions were obtained via cation-exchange and size-exclusion chromatography.

MT assembly

Tubulin samples were preincubated on ice for 5 min in polymerization buffer (50 mM MES-KOH pH 6.8, 50 mM KCl, 20% glycerol, 1 mM EGTA, 4 mM $MgCl_2$, 1 mM GTP) in the presence or absence of polyamines. Tubulin polymerization was then initiated by shifting the temperature to 37°C in an Ultrospec 3000 spectrophotometer (GE Healthcare, Fairfield, CT) equipped with a temperature controller. The kinetics of MT assembly was monitored by turbidimetry at 370 nm.

To study the sensitivity of MT samples to cold shock, two thermoregulated water pumps placed in different water baths were used. One was set to 37°C to start or resume MT polymerization. The second one, set at 10°C, was used to induce a brief cold shock. A 2-min cold shock was found to be a good compromise between a sufficient drop of the absorbance curve, for an easy detection, and a relatively small amount of MT depolymerization.

Atomic force microscopy

Ten microliters of tubulin or MT samples were deposited on freshly cleaved mica and dried for atomic force microscopy (AFM) imaging as described previously (18), the electrostatic adsorption of MTs on mica being mediated by the multivalent cations (magnesium, Spm). All AFM experiments were performed in intermittent mode with a multimode AFM instrument (Digital Instruments, Veeco, Santa Barbara, CA) operating with a Nanoscope IIIa controller (Digital Instruments). We used AC160TS silicon cantilevers (Olympus, Hamburg, Germany) with resonance frequencies of ~300 kHz. The applied force was minimized as much as possible. Images were collected at a scan frequency of 1.5 Hz and a resolution of 512 × 512 pixels.

RESULTS AND DISCUSSION

Spm induces MT bundling but not tubulin aggregation at physiological ionic strengths

Tubulin self-attraction can be mediated by cationic polyamines via their sharing between the highly negatively charged C-terminal tails of tubulin (Fig. 1 and (15)). However, due to the entropy penalty associated with tubulin aggregation, the weak attraction generated by polyamines at physiological ionic strengths is not expected to lead to the formation of large tubulin aggregates (see Text S1 in the Supporting Material for details). Using high resolution imaging, we controlled whether Spm triggers the formation of tubulin aggregates at near physiological ionic strengths ($I = 0.12$ M). To avoid the presence of MTs, the experiments were performed at low temperature (10°C) for which MTs cannot be assembled (Fig. 2 *A*). Even in the presence of Spm up to 3 mM, large aggregates were not detected by AFM on mica. However, we cannot exclude short chains of tubulin oligomers to be present in the bulk solution and to dissociate upon adsorption on mica. To confirm the nonformation of large tubulin aggregates, we measured the variations of tubulin sample absorbance with and without Spm (Fig. 2 *B*). At physiological ionic strength, the results clearly

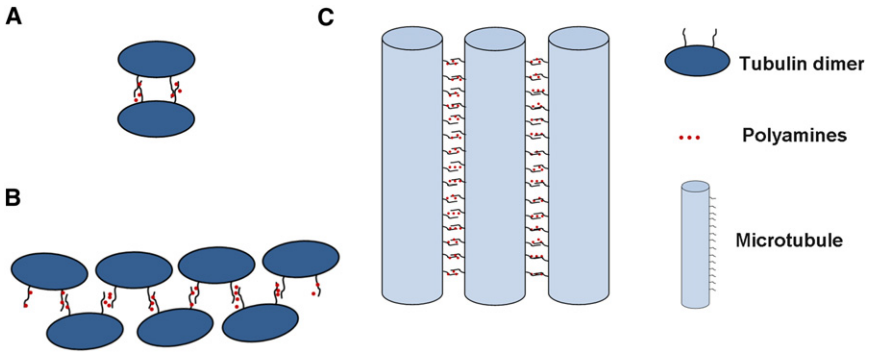

FIGURE 1 Schematic representations of putative tubulin configurations induced by polyamines. (*A*) Two dimers associate to form a tetramer. (*B*) Chain of tubulin dimers. (*C*) MT bundles.

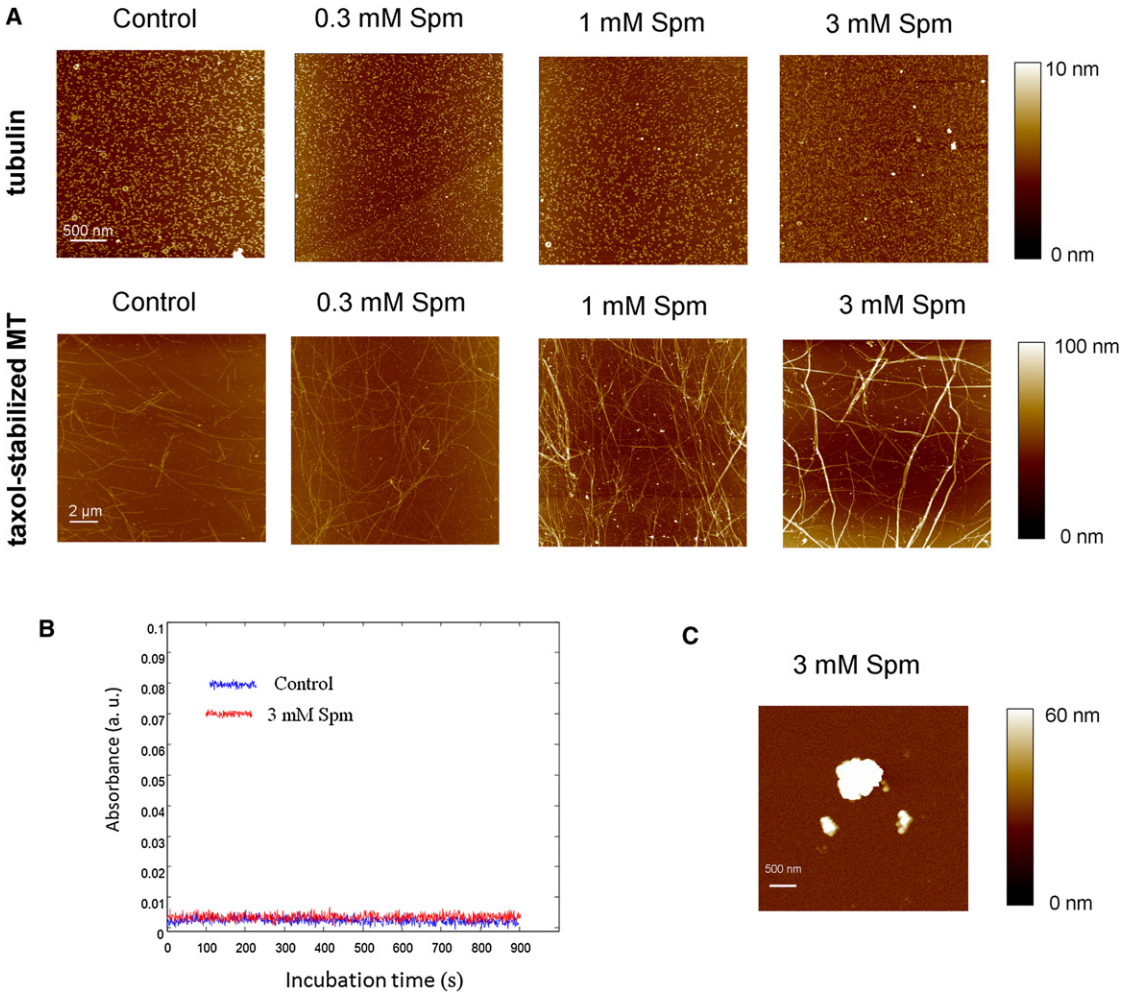

FIGURE 2 Spm favors MT bundling and does not aggregate tubulin at physiological ionic strengths. (*A*) AFM observation of samples containing unpolymerized tubulin (5 μM tubulin, 10°C), or taxol-stabilized MTs (5 μM tubulin, 2 μM taxol, 37°C) at varying concentrations of Spm. No aggregation was observed. All experiments were performed in 50 mM MES-KOH pH 6.8, 0.5 mM EGTA, 50 mM KCl, 4 mM $MgCl_2$, 1 mM GTP, 20% glycerol unless stated otherwise. Incubation time: 1 h. (*B*) Absorbance variations upon addition of 3 mM Spm to 10 μM free tubulin at 10°C to prevent MT polymerization. No variation of absorbance was detected over time in the presence of Spm. (*C*) At low ionic strength (25 mM MES-KOH pH 6.8, 0.5 mM EGTA, 4 mM $MgCl_2$, 1 mM GTP, 20% glycerol), 3 mM Spm leads to the formation of large tubulin aggregates (5 μM tubulin, 10°C).

show that Spm does not induce the formation of aggregates larger than the light wavelength. This is only true at moderate and high ionic strengths ($I > 0.1$M) because, when the experiments were performed without KCl ($I \sim 0.03$ M in 25 mM MES-KOH pH 6.8 and 3 mM Spm), we detected the presence of tubulin aggregates due to strong electrostatic attraction (Fig. 2 *C*, and (15)).

In contrast to the aggregation of free tubulin, MT bundling is considered as more favorable in the presence of Spm because tubulin dimers are immobilized in the MT wall (Fig. 1 and Text S1 in the Supporting Material for details). To test this hypothesis, we preformed taxol-stabilized MTs in the absence of Spm and analyzed by AFM the formation of MT bundles after the addition of Spm at varying concentrations for 1 h (Fig. 2 *A*). The results clearly indicate that Spm allows the formation of MT bundles at concentrations larger than 300 μM and increasing Spm concentration from 300 μM to 3 mM leads to the formation of even larger bundles, most probably to maximize the electrostatic benefit of polyamine sharing.

Kinetics of MT bundle assembly in the presence of Spm

In the most widely used model to describe MT assembly, a two-step mechanism is generally advanced (19,20). The first step, nucleation, involves the formation of critical size nuclei, containing few GTP-tubulin dimers, which are stable enough to allow the formation of short MTs (20). In the second step called elongation, MT growth results from the addition of GTP-tubulin dimers to MT ends.

MTs, in the absence of stabilizing factors, are highly dynamical polymers which frequently alternate between shortening and growth phases. In vitro, this behavior is

mainly governed by the supply of GTP-tubulin to microtubules (21,22). Below a critical GTP-tubulin concentration, C_c, which value depends on the buffer conditions (~18 μM for control and ~10 μM with 1 mM Spm), the supply of GTP-tubulin is not sufficient to sustain MT assembly. The C_C can also be regarded as the pool of free GTP-tubulin in equilibrium with MTs at steady state. The assembly of tubulin into MTs can be monitored by turbidity, which generally reflects the amount of MTs versus time after an ice-cold tubulin sample is placed in a prewarmed spectrophotometer cuvette. Albeit very useful, the absorbance value needs to be considered with cautions because MT bundles diffract light with a better efficiency than do isolated MTs and the relation between absorbance and MT mass is then no longer linear (23). For this reason, we combined AFM data with turbidity measurement to understand the mechanism of MT assembly in the presence of Spm and to access the nature of objects which diffracted light.

Tubulin assembly in the presence of Spm leads to the rapid formation of short MT bundles

Tubulin assembly was monitored by turbidimetry measurement at 37°C in the presence or absence of Spm (Fig. 3 *A*). The assembly curves displayed typical patterns of MT polymerization with a flat plateau in the absence or presence of Spm up to 1 mM. At 3 mM Spm, the plateau was no longer stable thus indicating aggregation or bundling at a slow rate (data not shown). Two important points deserve to be noticed.

First, both the lag time and the time required to reach the plateau value are shorter in the presence of Spm—thus indicating higher rates of nucleation and elongation, respectively, as measured under nonbundling conditions with Spm (15).

Second, the plateau value significantly increases in the presence of Spm and, owing to the magnitude of this increase (~8 times for 1 mM Spm compared to control), a higher amount of polymerized MTs cannot solely account for this phenomenon (Fig. S1 *A* in the Supporting Material). To further explore this point, we analyzed the power law dependence of the sample absorbance (Fig. S1 *B*), ΔA, on light wavelength, λ: $\Delta A \sim \lambda^{-n}$ (24). For isolated MTs (i.e., without Spm) $n \sim 3.1$, which corresponds to light diffraction by thin rods ($n = 3$). This is in agreement with the Berne turbidity criterion, which states that the absorbance and MT concentration are directly proportional (23). However, in the presence of Spm, we observed a significant decrease of n (from 3.1 to 1.7 for 0–3 mM Spm). Together, these results indicate that the tubulin polymers by which light was diffracted in the presence of Spm were no longer thin rods like MTs but were aggregates of diverse structures (25) or bundles. AFM results strongly favor the latter hypothesis, as MT bundles were detected on mica rather than large aggregates (Fig. 3 *B*). MT bundling thus appears as the most rational explanation to account for the higher plateau value of the assembly curve. In Fig. 3 *B*, we also noticed that thicker and shorter bundles were formed at higher Spm concentrations, in agreement with a decreasing n value (Fig. S1 *B*).

We then explored whether forces other than electrostatic origin participate in MT bundling. For this purpose, the strength of the electrostatic force was decreased by increasing the ionic strength. In agreement with our hypothesis of an electrostatic-mediated bundling, an increase of

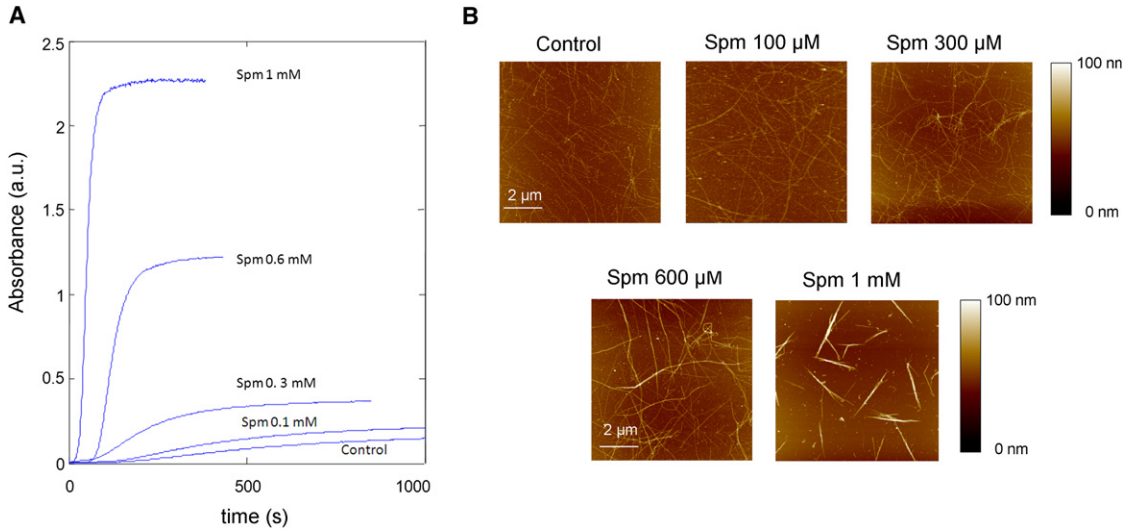

FIGURE 3 Tubulin assembly in the presence of Spm leads to formation of short bundles. (*A*) Tubulin assembly assessed by turbidity ($\lambda = 370$ nm) for various Spm concentrations (25 μM tubulin). We remark that both the lag time to start polymerization and the time required to reach the plateau shorten as Spm concentration increases. (*B*) AFM images of MTs assembled for 30 min at 37°C in the presence of varying concentrations of Spm (25 μM tubulin). MT bundles are clearly detected at 300 μM Spm and at higher concentrations.

ionic strength caused the assembly of longer MTs and thinner bundles (Fig. S2) and, at ionic strengths higher than 200 mM for 1 mM Spm, only isolated MTs were detected by AFM.

In another important control, we investigated whether MTs can be released from bundles and were not irreversibly bound to it. To induce MT release from bundles, we added KCl by successive 100 mM steps up to 300 mM to a solution containing preformed MT bundles (Fig. S3 *A*). MT bundles were first stabilized with taxol to prevent their depolymerization under such conditions. Upon KCl addition, we observed a decrease of absorbance with time to reach a lower plateau value roughly corresponding to that obtained when MTs were assembled in the absence of Spm. This result is in agreement with the release of MTs from bundles in bulk solution, thus leading to isolated MTs. Finally, we observed by AFM that short and isolated MTs were indeed present at the end of the releasing process (Fig. S3 *B*).

Scaling laws for MT bundling

To provide further insights into how Spm favors the rapid formation of bundles, we performed time-lapse imaging of tubulin assembly by AFM together with analysis of the length and height distributions of MT bundles at various times (Fig. 4, *A* and *B*). After only 20 s (the shortest time that we can reasonably tackle by AFM), MT bundles of a few micrometers long were already formed in the presence of 1 mM Spm, whereas no MTs were present in control for the same incubation time. This result indicates that nucleation, elongation, and MT bundling occur at high rates in the presence of Spm. Interestingly, turbidimetry experiments show that when MTs were first formed under control conditions, the increase of absorbance upon addition of Spm was very slow if any, which indicates that MT bundling is inhibited for long MTs (Fig. 4 *C*). Let us advance some explanations to understand how MT bundles could be assembled from free tubulin and Spm so rapidly.

Short but not long MTs rapidly form bundles due to hindered diffusion

After nucleation, short MTs may diffuse in the bulk solution until collision with another one takes place to potentially form a bundle made of two MTs and so on. The orientationally average translational diffusion constant of rods, D_t, scales like

$$\frac{K_B T\, ln\left(\frac{L}{2R}\right)}{3\pi\eta L}, \qquad (1)$$

where η is the medium viscosity (~1 mPa.s for 20% glycerol at 300 K) and, R and L are the radius and length of the rods, respectively (26,27). If we assume that MTs could potentially undergo collision whenever their separation distance is shorter than their length, the time between collision is $t_c \sim 1/4\pi D_t C_{MT} L$, where C_{MT} is the MT concentration. The generalization to bundles containing N MTs of mean length L leads to

$$t_c \sim \frac{N}{4\pi D_t C_{MT} L} \sim \frac{3N\eta}{4K_B T\, ln\left(\frac{L}{2R}\right) C_{MT}}, \qquad (2)$$

with R scaling like $\sqrt{N}a$, a being the MT radius (a~12 nm). For $N = 0$ and $C_{MT} = 6.10^{-10}$ M, we obtain $t_c \sim 1$ s with $L = 10\,\mu$m and $t_c \sim 1.9$ s with $L = 1\,\mu$m. Bundles should then coalesce rapidly and MT length should then little affect t_c because the slower diffusion of long MTs is compensated by a larger explored volume. This is true provided that the search due to MT rotation is significantly faster than translational diffusion. Let us consider this point in further detail. The mathematical expression of rod rotational diffusion, D_R, is

$$\frac{3K_B T\, ln\left(\frac{L}{2R}\right)}{\pi\eta L^3} \text{ in rad}^2/\text{s}. \qquad (3)$$

The rotational diffusion is then highly sensitive to L as D_R scales like $ln(L)/L^3$. For bundles containing 1-μm-long MTs and $N = 10$, the time required, Δt, to obtain a rotation angle of $\Delta\theta = \pi/2$, using $\Delta\theta \sim \sqrt{4D_R\Delta t}$, is <60 ms, whereas >30 s are necessary for the same rotation amplitude with 10-μm-long MTs. Even though, as reported previously for actin filaments (26), the negative effect of increasing L on diffusion can be partly compensated by an expansion of the capture region with L, rotation is clearly the rate-limiting step for the formation of bundles made of long MTs as soon as L exceeds few micrometers. In light of these scaling considerations, we understand the rapid bundle assembly from freshly nucleated and short MTs. Accordingly, we report that, to form thick MT bundles from preformed MTs, the sample needs to be vortexed to shorten MTs or favor diffusion (Fig. S4).

Spm could potentially promote nucleation of parallel MTs or induce MT self-nucleation properties

The obstacle of rotational diffusion to MT bundles can also be overcome if parallel MTs are nucleated simultaneously from large oligomers containing multiple nuclei, or if MTs promote the formation of nucleus on their surface. In agreement with this, Spm may lead to the self-attraction of tubulin oligomers (nucleus) or to the attraction of tubulin dimers on the MT wall. However, both nucleation of multiple MTs from large oligomers or MT self-nucleation may lead to the rapid assembly of short MT bundles which can be hardly distinguished from MT bundles generated by rapid diffusion of short and isolated MTs (<μm). Further work deserves to be done in that direction.

Apparent finite height of MT bundles

The analysis of AFM data shows that, for incubation times longer than 20 s, the length of MT bundles gradually

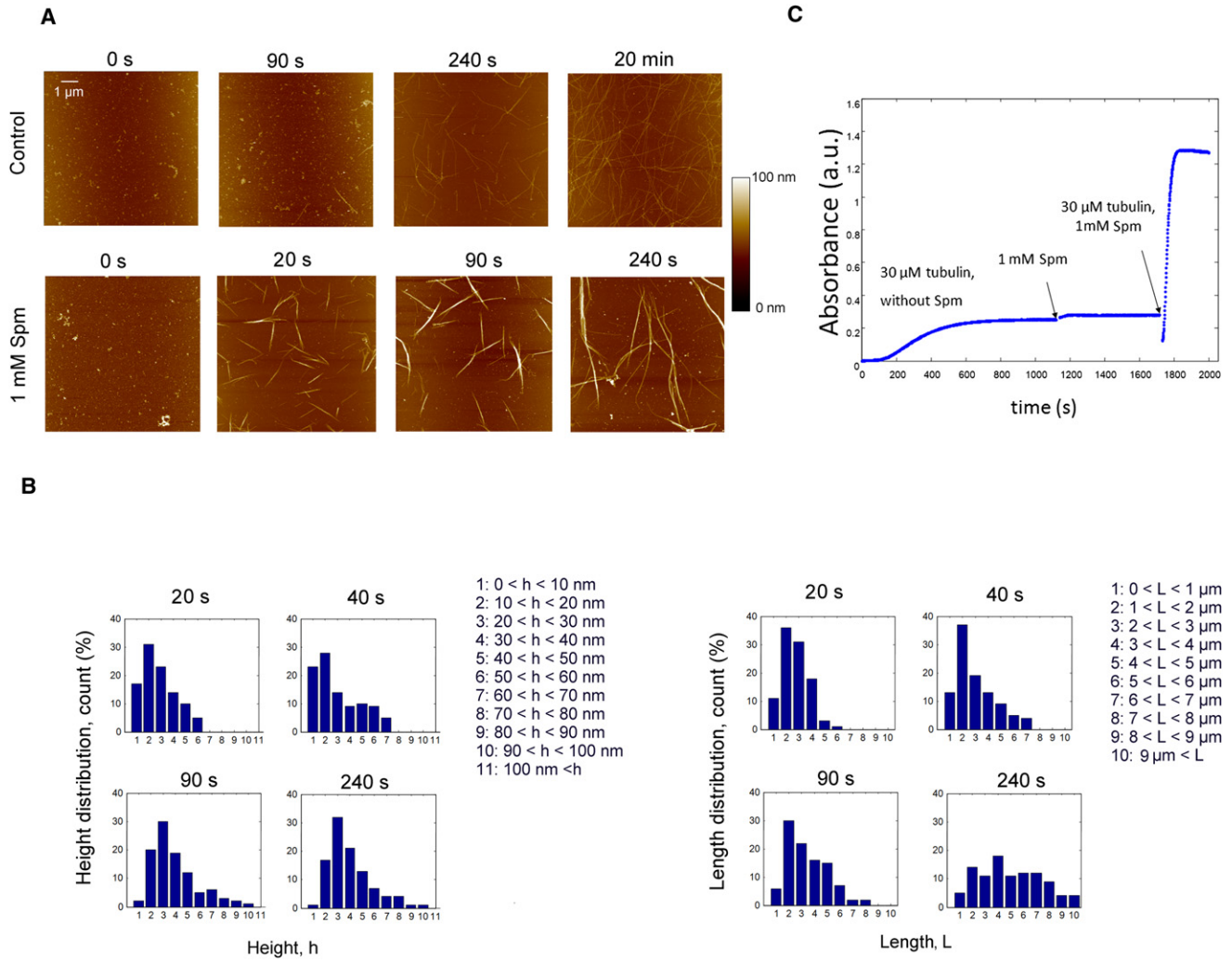

FIGURE 4 Kinetics of bundle formation: short MTs are necessary for rapid bundle assembly. (*A*) AFM images of tubulin (30 μM) assembly into MT bundles at various times. Aliquots were imaged from the same assembly mix in each condition. We noted that rather short MT bundles appeared in 20 s in the presence of Spm whereas no MTs were observed before 90 s of incubation without Spm. (*B*) Statistical analysis of the time evolution of bundle heights and lengths over 300 MT bundles assembled in the presence of 1 mM Spm. The height distribution of MT bundles remains unchanged for times longer than 90 s. On the other hand, the length distribution of MT bundles flattens out over time. The AFM measurements reflect the thickness of bundles but could not be used to quantify the number of MTs per bundle. (*C*) 30 μM tubulin was first allowed to polymerize to form long MTs in the absence of Spm, then, 1 mM Spm was added. Interestingly, contrary to what expected for bundling, the absorbance value only slightly increased. Finally, we injected an equal volume of 30 μM ice-cold tubulin with 1 mM Spm to the warmed cuvette containing the MT solution. We noticed that the absorbance drops to half its preceding value, owing to the two-times MT dilution, and then very rapidly raised up to four times its value before dilution. This experiment clearly indicates that newly formed short MTs can be assembled into thick bundles, in contrast to long MTs.

increased and the length distribution had a tendency to flatten out over time (Fig. 4 *B*), probably via the addition of the remaining tubulin dimers to the ends of MTs in the bundles. The lengthening of bundles over time also indicates that bundles are dynamical structures, for which elongation benefits from MT catastrophes. On the other hand, we obtained a rather stable peak distribution of bundle height for long incubation times (>90 s; Fig. S5), in agreement with the stable plateau value of the absorbance curve (Fig. 4 *B*).

This result indicates that self-association between bundles occurred at a low rate for longer incubation times. Several hypotheses can be put forward to explain such phenomenon. As reported for actin, a frustration of the bundling mechanism can occur due to a mechanical penalty like the twist of actin filaments (28). However, the nature of a putative frustration mechanism remains to be identified for MT bundling. Using our model, we can also propose an interesting alternative. As rotational movements are rate-limiting for bundling, MT elongation leads to longer bundles and then considerably decreases the bundling rates. In addition to this, MTs were recently shown to form a three-dimensional mesh in bulk solution, with characteristic length of

$$\zeta \sim \frac{1\mu\text{m}}{\sqrt{C_{pol}}}, \tag{4}$$

where C_{pol} is the concentration of polymerized tubulin in mg/ml (29). We can extend this relation to bundles comprising N MTs, $\zeta \sim 1\mu\text{m}/\sqrt{C_{pol}/N}$, in which we note that the mesh enlarges due to MT bundling. During MT elongation, bundles longer than ζ are trapped in this mesh, which precludes further bundling. The bundling process should then take place before MTs reached this critical length. For 10 μM of polymerized tubulin (1.1 mg/ml) and $N = 10$, we obtain $\zeta \sim 3$ μm. If we assume that the MT growth rates range from 2 to 6 μm/min in vitro, bundling should stop 30–90 s after the beginning of polymerization, as observed by AFM in the presence of 1 mM Spm (Fig. 4 *B*).

High sensitivity of MT bundles to cold shock: a collective behavior

To explore the dynamical properties of MT bundles, we studied their sensitivity to a brief cold shock by turbidimetry (Fig. 5 *A*). As a first control, we observed that 5 μM taxol was sufficient to prevent bundles from depolymerizing under cold shock and, importantly, the absorbance remained at the plateau value with little perturbations (Fig. 5 *B*). This experiment indicates that low temperatures do not induce the release of MTs from bundles, which would have decreased the absorbance value. We then performed a series of experiments to analyze, at various Spm concentrations, the responses of isolated MTs and MT bundles to cold shock (Fig. 5 *C*). Whereas, in the absence of Spm, we scarcely noted a variation of absorbance upon a brief exposure to cold, Spm-mediated MT bundles were more and more

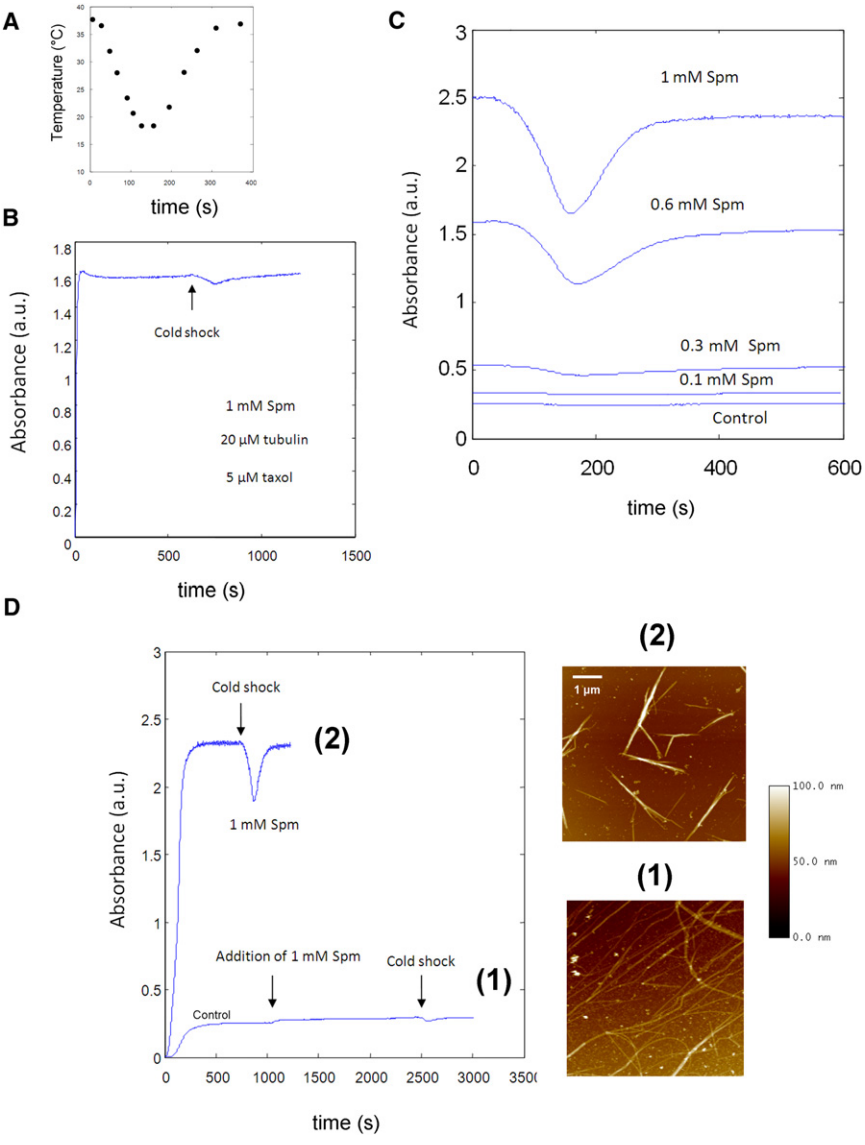

FIGURE 5 MT bundles display a higher sensitivity than MTs to brief cold shock. (*A*) Temperature variations inside the spectrophotometer cuvette versus time after 2 min cold exposure. (*B*) Taxol-stabilized MTs are not released from bundles upon 2-min cold exposure. When cold exposure was applied to taxol-stabilized bundles formed in the presence of Spm, only a small absorbance variation was observed during cold shock. (*C*) Absorbance variations of MTs versus Spm concentration. A quantity of 30 μM tubulin was allowed to polymerize in the absence or presence of Spm. When the absorbance reached its plateau value, a brief cold shock was applied to the sample (see (*A*)). (*D*) When 1 mM Spm was added to a solution containing preformed MTs (30 μM tubulin), bundling was hindered and the sensitivity to the short cold shock significantly decreased. AFM imaging showed that isolated MTs or thin bundles (*1*) were present under such conditions, whereas thick and short bundles were formed when Spm was present from the beginning of tubulin polymerization (*2*).

sensitive to cold shock when the Spm concentration increased from 0.3 to 1 mM.

To explore whether this behavior was due to MT bundling and not only to the sole presence of Spm, we compared the sensitivity of short bundles assembled in the presence of 1 mM Spm to that of isolated MTs for which Spm was added after their polymerization. In the latter case, MT bundling is inhibited by hindered diffusion (Fig. 5 *D*) and we observed a lack of sensitivity to cold shock, whereas thick and short bundles displayed a high sensitivity. Consequently, the sensitivity of MTs is not simply due to the presence of Spm but, instead, to MT bundling.

To understand what could account for this phenomenon, we investigated the relationships between cold sensitivity and tubulin concentration both for isolated MTs and bundles. For isolated MTs, as already advanced to explain the phenomenon of MT oscillations ((30,31), see Text S2 in the Supporting Material), the presence of GDP-rings made of GDP-tubulin dimers can account for the increased sensitivity of MTs to cold exposure (Fig. 6, *A–C*). However, in contrast with isolated MTs, the sensitivity of MT bundles to cold exposure does not increase with tubulin concentration (Fig. 6, *A–C*). Such behavior may be explained by a collective behavior of MTs within bundles.

Indeed, as already reported for MT growing from axonemes (14), the destabilization of one MT in a bundle may increase the probability for other MTs in the same bundle to undergo catastrophes. To further explore the putative implication of GDP-rings in MT bundle reactivity, we performed high-resolution AFM imaging of MT samples after a brief cold shock (1 min at 10°C, Fig. 7 *A*). Without Spm, we observed short oligomers and a few rings at the ends of MTs, whereas, in the presence of 1 mM Spm, large clusters of GDP-tubulin rings were detected being most probably the product of bundle disassembly. As expected with Spm, neutralization of the tubulin C-terminal tails is known to favor the formation of GDP-tubulin rings (32). Interestingly, at the ends of some MTs, we also noted that tubulin rings tend to be aligned along MT walls. Altogether, these results thus suggest that GDP-tubulin rings should play a key role in bundle sensitivity to cold shock.

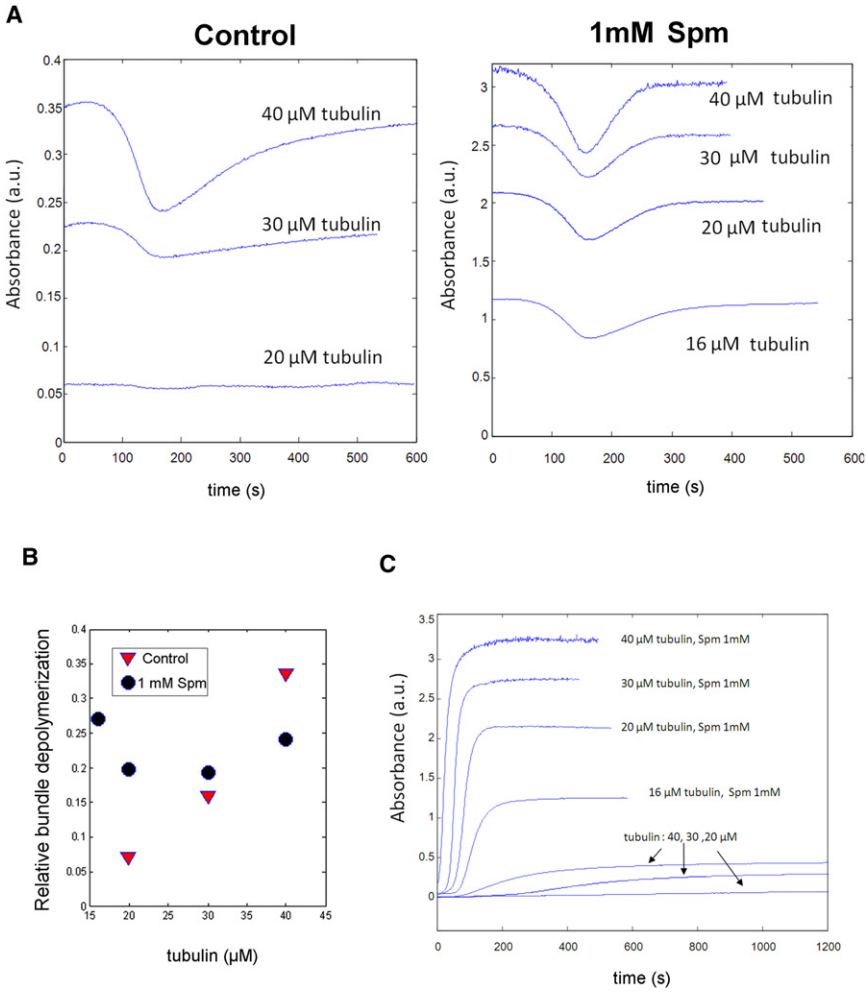

FIGURE 6 Sensitivity of MT bundles to brief cold exposure reveals a collective behavior. (*A*) MT sample responses to the 2-min cold shock (as shown in Fig. 5 *A*) applied after reaching the plateau value of tubulin assembly. In the presence of Spm, the absorbance drop was of large amplitude whatever the tubulin concentration, while, for control, the sensitivity of isolated MTs to cold shock was highly sensitive to tubulin concentration. (*B*) Relative depolymerization upon cold exposure, which is the ratio of the amplitude of the absorbance drop to the plateau value. (*C*) Assembly curves from which MT sensitivity to cold exposure was tested (*A*).

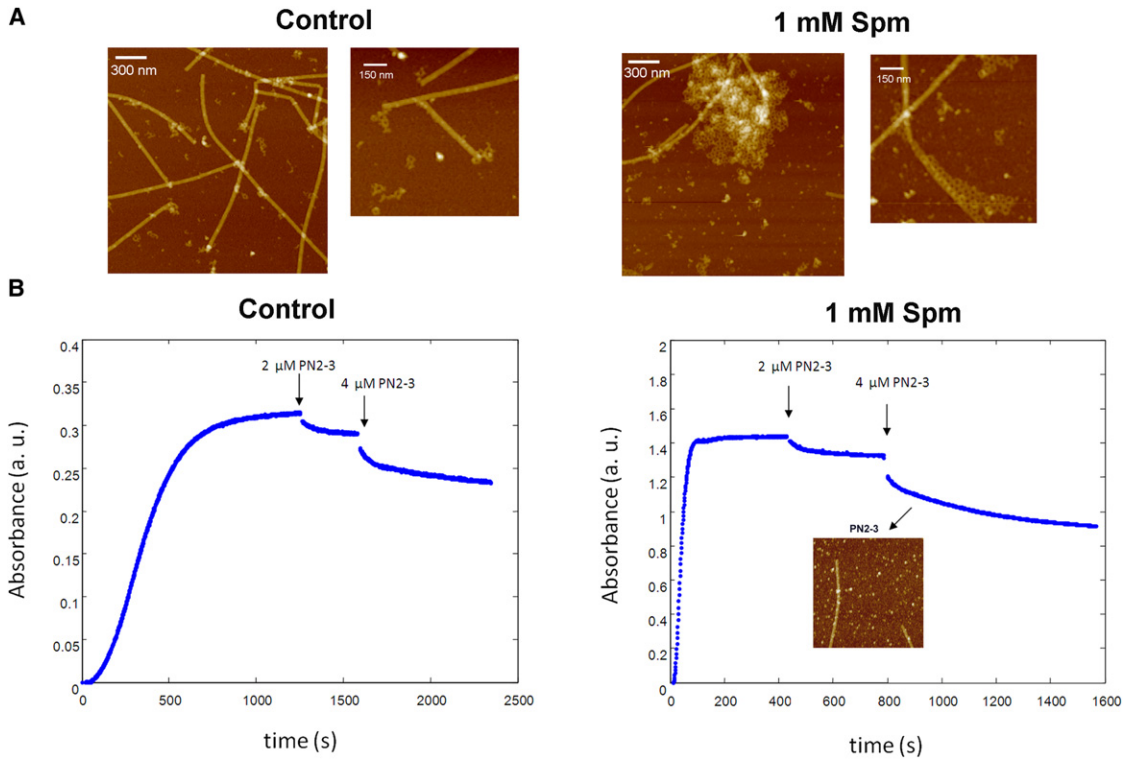

FIGURE 7 Cold destabilization of MTs in the presence of Spm leads to the formation of arrays of GDP-tubulin rings which mediate the higher MT bundle reactivity. (*A*) AFM imaging of MT cold destabilization (1 min) in the presence or absence of 1 mM Spm. In control, we observed small oligomeric structures and broken rings at the ends of destabilized MTs. On the other hand, in the presence of 1 mM Spm, large arrays of rings were clearly observed. 25 μM tubulin. (*B*) MTs were destabilized by successive additions of PN2-3, a destabilizing agent, in the presence or absence of Spm. The reactivity of MTs to PN2-3 did not significantly increase in the presence of bundles. The AFM image shows that, even in the presence of Spm, MT disassembly due to PN2-3 did not lead to the production of GDP-tubulin rings. 25 μM tubulin.

Low reactivity of MT bundles upon PN2-3-mediated destabilization

PN2-3 is a protein fragment from CPAP, a centrosomal protein, displaying a significant MT-destabilization activity (33,34). It was shown that MT destabilization by PN2-3 can result either from the sequestration of tubulin in a 1:1 PN2-3/tubulin complex (34) or from the ability of PN2-3 to directly destabilize MTs, as it can depolymerize taxol-stabilized MTs. The point of using PN2-3 to destabilize MTs is that, in contrast to cold exposure, PN2-3 does not lead to the formation of GDP-tubulin ring intermediates (Fig. 7 *B*), most probably because the binding of PN2-3 to tubulin is not compatible with ring formation. Interestingly, when PN2-3 was added at low concentrations to induce MT destabilization, we did not observe a significant difference of sample reactivity for isolated or bundled MTs (Fig. 7 *B*). In agreement with our model, the formation of GDP-tubulin oligomers or rings upon MT destabilization is then a prerequisite for a collective behavior of bundled MTs to take place.

Scaling considerations for bundle sensitivity to cold exposure

Let us consider, N, the number of MTs per bundle, with J_s as the dissociation rate of tubulin dimers and D_{ring} as the coefficient of diffusion for GDP-tubulin rings. To evaluate whether a collective behavior in MT bundles may occur, we estimate to which extent one MT undergoing catastrophe increases the concentration of GDP-tubulin near other MTs within the same bundle. When the MT-ends emerge from the bundle tip, we assume that, in agreement with AFM observations, no sterical hindrance due to the presence of nearest MTs prevents the formation of GDP-tubulin oligomers upon MT destabilization. The separation distance, l, between two nearest MT ends at the bundle tip, if they are aligned, scales like σ/N where σ is the variance of MT length. Then, the relative concentration of freshly released GDP-tubulin to that of free GTP-tubulin (C_c) at the nearest MT ends in the bundle is (obtained by substituting l with σ/N and D_{tub}, the tubulin diffusion constant, with D_{ring}, the GDP-tubulin ring diffusion constant, in Eq. 2, Text S2 in the Supporting Material):

$$\nu \sim \frac{NJ_s}{\sigma D_{ring}} / C_c. \tag{5}$$

The value ν reflects the probability for GDP-tubulin, here in the form of rings, to pollute the nearest microtubule ends and then to induce catastrophe. Thus, $\nu \sim 0.27$ in the case

of thick MT bundles with $\sigma \sim 2\ \mu m$, $N = 30$, $C_c \sim 10\ \mu M$ (1 mM Spm), $D_{ring} = 5\ \mu m^2/s$ (35) and a dissociation rate of GDP-tubulin, J_s, of 546 dimers/s, while, for thinner and longer bundles, $\nu \sim 5.4\ 10^{-3}$ with $\sigma \sim 10\ \mu m$, $N = 3$. Within short and thick MT bundles, ν is then significantly higher than for thinner and longer ones, which may promote a collective behavior using GDP-tubulin rings as vehicles. In line with this, at lower Spm concentrations, thinner and longer bundles were observed and their sensitivity to cold exposure decreased (see Fig. 3 *B* for AFM imaging and Fig. 5 *C* for bundle reactivity). Finally, as expected from our results (Fig. 6 *A*), ν for MT bundles does not depend on the total tubulin concentration in contrast with isolated microtubules (see Text S2 in the Supporting Material).

Extensions to in vivo conditions

Polyamines are present at millimolar concentrations in living cells (16,36) and changes in their levels are known to reorganize the cell cytoskeleton. Polyamines promote actin polymerization (37) and bundling in vitro (38) and may play a role in actin dynamics and architecture in vivo. In cells, it was shown that polyamine depletion induces the reorganization of the actin filaments and the disappearance of actin stress fibers (39), such effects being attributed to the inactivation of proteins of the Rho family such as Rac1, which regulates the organization of the actin cytoskeleton (40).

Polyamines were also shown to interact, directly and (or) indirectly, with MTs in cells (41–43) but little is known regarding their potential influence on MT bundle functions. In cells and especially in neurons, polyamines are probably not necessary to form MT bundles as specialized MAPs like Tau have the ability to stabilize and cross-link MTs into thick bundles. However, in light of the results summarized in Fig. 8, one may wonder if polyamines can modulate the dynamical properties of MT bundles. Among natural polyamines, only spermidine and Spm but not putrescine can favor MT bundling at physiological ionic strengths. In line with this, changes in polyamine levels promote axon branching and neuritic outgrowth in neurons (44,45). Such effects may be due to the binding of polyamines to the C-terminal tails of tubulin, as already suggested (46).

In addition, many theoretical arguments indicate that natural polyamines are good candidates as counterions to neutralize the C-terminal tail of tubulin (15). Our results demonstrate that Spm, at near-physiological ionic strengths, promotes the formation of MT bundles whereas no aggregation of free tubulin dimers into large structures was detected under similar conditions (Fig. 2). This property can be of great interest in vivo. Indeed, tubulin aggregation would have a disastrous effect in cells because GTP-tubulin diffusion to MT-ends would have been hindered, thus inhibiting MT polymerization. The two C-terminal tails of tubulin dimers are known to play the role of anchors for MAPs and at least one of them is necessary to maintain normal

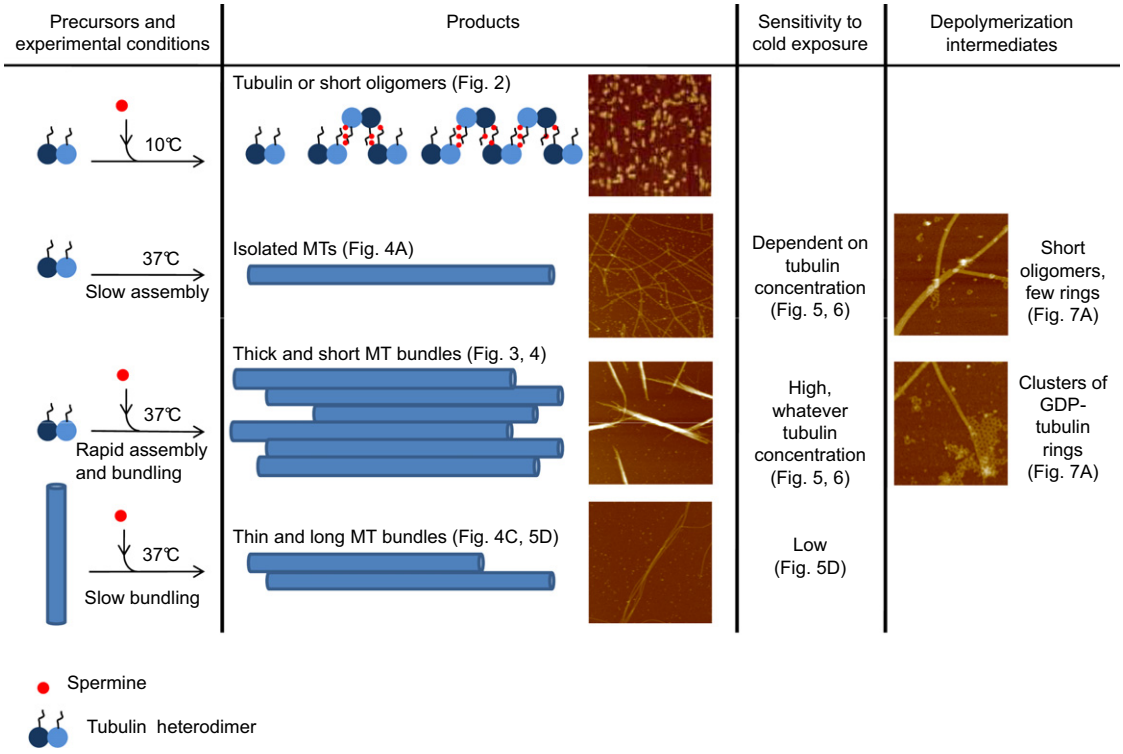

FIGURE 8 Schematic representation of the major experimental results.

MT function in cells (47). In addition to this, we may also propose that tubulin C-terminal tails serve to preclude the formation of tubulin aggregates.

In many cases, MT bundles in vivo are nonpermanent structures which undergo rapid assembly and disassembly. MT bundle dynamics is necessary in neurons for axon branching (48,49), growth cone turning (50), dendritic spin protrusions (51) but also in other organisms as for hyphal branching in fungi (52). Interestingly, whenever MT bundles should change their orientation to explore a new space, short MTs come into play (51). Our experimental results suggest that short MT bundles display interesting dynamical properties with a higher sensitivity to brief cold exposure than bundles made of long MTs. Along with this, MT severing proteins in neurons such as katanin and spastin allow the local production of free tubulin as a result of MT disassembly. Such supply of free tubulin may support the growth of many critical nuclei and then lead to the assembly of highly reactive short MT bundles.

Even though defects in polyamine metabolism may be implicated in cerebellar circuitry dysfunctions such as mental retardation (53), suicide (54), and altered brain morphology (55), little is known regarding the role of polyamines in the brain. So far, polyamines were thought to modulate functions related to ion channels (53). However, our study indicates that polyamines may also participate in other neuron functions via their impact on the dynamical properties of MT bundles.

SUPPORTING MATERIAL

Supplementary Figs. 1–5 and Text 1 and 2 are available at http://www.biophysj.org/biophysj/supplemental/S0006-3495(11)00592-3.

This work was supported by funds from the Institut National de la Santé et de la Recherche Médicale. We gratefully acknowledge the Genopole EVRY for constant support of the laboratory.

REFERENCES

1. Wittmann, T., A. Hyman, and A. Desai. 2001. The spindle: a dynamic assembly of microtubules and motors. *Nat. Cell Biol.* 3:E28–E34.
2. Holy, T. E., M. Dogterom, …, S. Leibler. 1997. Assembly and positioning of microtubule asters in microfabricated chambers. *Proc. Natl. Acad. Sci. USA.* 94:6228–6231.
3. Faivre-Moskalenko, C., and M. Dogterom. 2002. Dynamics of microtubule asters in microfabricated chambers: the role of catastrophes. *Proc. Natl. Acad. Sci. USA.* 99:16788–16793.
4. Tabony, J. 2006. Microtubules viewed as molecular ant colonies. *Biol. Cell.* 98:603–617.
5. Liu, Y., Y. Guo, …, J. X. Tang. 2006. Microtubule bundling and nested buckling drive stripe formation in polymerizing tubulin solutions. *Proc. Natl. Acad. Sci. USA.* 103:10654–10659.
6. Mandelkow, E., E. M. Mandelkow, …, S. C. Müller. 1989. Spatial patterns from oscillating microtubules. *Science.* 246:1291–1293.
7. Nédélec, F., T. Surrey, and E. Karsenti. 2003. Self-organization and forces in the microtubule cytoskeleton. *Curr. Opin. Cell Biol.* 15:118–124.
8. Papaseit, C., N. Pochon, and J. Tabony. 2000. Microtubule self-organization is gravity-dependent. *Proc. Natl. Acad. Sci. USA.* 97:8364–8368.
9. Tabony, J., N. Glade, …, J. Demongeot. 2002. Microtubule self-organization and its gravity dependence. *Adv. Space Biol. Med.* 8:19–58.
10. Glade, N., and J. Tabony. 2005. Brief exposure to high magnetic fields determines microtubule self-organization by reaction-diffusion processes. *Biophys. Chem.* 115:29–35.
11. Kanai, Y., R. Takemura, …, N. Hirokawa. 1989. Expression of multiple tau isoforms and microtubule bundle formation in fibroblasts transfected with a single tau cDNA. *J. Cell Biol.* 109:1173–1184.
12. Lee, G., and S. L. Rook. 1992. Expression of tau protein in non-neuronal cells: microtubule binding and stabilization. *J. Cell Sci.* 102:227–237.
13. Takemura, R., S. Okabe, …, N. Hirokawa. 1992. Increased microtubule stability and α-tubulin acetylation in cells transfected with microtubule-associated proteins MAP1B, MAP2 or tau. *J. Cell Sci.* 103: 953–964.
14. Laan, L., J. Husson, …, M. Dogterom. 2008. Force-generation and dynamic instability of microtubule bundles. *Proc. Natl. Acad. Sci. USA.* 105:8920–8925.
15. Mechulam, A., K. G. Chernov, …, D. Pastré. 2009. Polyamine sharing between tubulin dimers favors microtubule nucleation and elongation via facilitated diffusion. *PLOS Comput. Biol.* 5:e1000255.
16. Thomas, T., and T. J. Thomas. 2003. Polyamine metabolism and cancer. *J. Cell. Mol. Med.* 7:113–126.
17. Chernov, K. G., A. Mechulam, …, P. A. Curmi. 2008. YB-1 promotes microtubule assembly in vitro through interaction with tubulin and microtubules. *BMC Biochem.* 9:23.
18. Chernov, K. G., P. A. Curmi, …, D. Pastré. 2008. Atomic force microscopy reveals binding of mRNA to microtubules mediated by two major mRNP proteins YB-1 and PABP. *FEBS Lett.* 582:2875–2881.
19. Voter, W. A., and H. P. Erickson. 1984. The kinetics of microtubule assembly. Evidence for a two-stage nucleation mechanism. *J. Biol. Chem.* 259:10430–10438.
20. Flyvbjerg, H., E. Jobs, and S. Leibler. 1996. Kinetics of self-assembling microtubules: an "inverse problem" in biochemistry. *Proc. Natl. Acad. Sci. USA.* 93:5975–5979.
21. Hinow, P., V. Rezania, and J. A. Tuszyński. 2009. Continuous model for microtubule dynamics with catastrophe, rescue, and nucleation processes. *Phys. Rev. E.* 80:031904.
22. Fygenson, D. K., E. Braun, and A. Libchaber. 1994. Phase diagram of microtubules. *Phys. Rev. E.* 50:1579–1588.
23. Berne, B. J. 1974. Interpretation of the light scattering from long rods. *J. Mol. Biol.* 89:755–758.
24. Andreu, J. M., and S. N. Timasheff. 1982. Tubulin bound to colchicine forms polymers different from microtubules. *Proc. Natl. Acad. Sci. USA.* 79:6753–6756.
25. Unger, E., K. J. Böhm, and W. Vater. 1986. Factors regulating microtubule structure—a minireview. *Acta Histochem. Suppl.* 33:85–94.
26. Yu, X., and A. E. Carlsson. 2004. Kinetics of filament bundling with attractive interactions. *Biophys. J.* 87:3679–3689.
27. Allison, S., C. Chen, and D. Stigter. 2001. The length dependence of translational diffusion, free solution electrophoretic mobility, and electrophoretic tether force of rigid rod-like model duplex DNA. *Biophys. J.* 81:2558–2568.
28. Claessens, M. M., C. Semmrich, …, A. R. Bausch. 2008. Helical twist controls the thickness of F-actin bundles. *Proc. Natl. Acad. Sci. USA.* 105:8819–8822.
29. Lin, Y.-C., G. H. Koenderink, …, D. A. Weitz. 2007. Viscoelastic properties of microtubule networks. *Macromolecules.* 40:7714–7720.
30. Melki, R., M. F. Carlier, and D. Pantaloni. 1988. Oscillations in microtubule polymerization: the rate of GTP regeneration on tubulin controls the period. *EMBO J.* 7:2653–2659.

31. Mandelkow, E. M., G. Lange, …, E. Mandelkow. 1988. Dynamics of the microtubule oscillator: role of nucleotides and tubulin-MAP interactions. *EMBO J.* 7:357–365.

32. Nicholson, W. V., M. Lee, …, E. Nogales. 1999. Cryo-electron microscopy of GDP-tubulin rings. *Cell Biochem. Biophys.* 31:175–183.

33. Hsu, W. B., L. Y. Hung, …, T. K. Tang. 2008. Functional characterization of the microtubule-binding and -destabilizing domains of CPAP and d-SAS-4. *Exp. Cell Res.* 314:2591–2602.

34. Cormier, A., M. J. Clément, …, P. A. Curmi. 2009. The PN2-3 domain of centrosomal P4.1-associated protein implements a novel mechanism for tubulin sequestration. *J. Biol. Chem.* 284:6909–6917.

35. Palmer, G. R., D. C. Clark, …, D. B. Sattelle. 1982. A quasi-elastic laser light scattering study of tubulin and microtubule protein from bovine brain. *J. Mol. Biol.* 160:641–658.

36. Watanabe, S., K. Kusama-Eguchi, …, K. Igarashi. 1991. Estimation of polyamine binding to macromolecules and ATP in bovine lymphocytes and rat liver. *J. Biol. Chem.* 266:20803–20809.

37. Oriol-Audit, C. 1978. Polyamine-induced actin polymerization. *Eur. J. Biochem.* 87:371–376.

38. Grant, N. J., C. Oriol-Audit, and M. J. Dickens. 1983. Supramolecular forms of actin induced by polyamines; an electron microscopic study. *Eur. J. Cell Biol.* 30:67–73.

39. McCormack, S. A., R. M. Ray, …, L. R. Johnson. 1999. Polyamine depletion alters the relationship of F-actin, G-actin, and thymosin β4 in migrating IEC-6 cells. *Am. J. Physiol.* 276:C459–C468.

40. Vaidya, R. J., R. M. Ray, and L. R. Johnson. 2005. MEK1 restores migration of polyamine-depleted cells by retention and activation of Rac1 in the cytoplasm. *Am. J. Physiol. Cell Physiol.* 288:C350–C359.

41. Savarin, P., A. Barbet, …, D. Pastré. 2010. A central role for polyamines in microtubule assembly in cells. *Biochem. J.* 430:151–159.

42. Pohjanpelto, P., I. Virtanen, and E. Hölttä. 1981. Polyamine starvation causes disappearance of actin filaments and microtubules in polyamine-auxotrophic CHO cells. *Nature.* 293:475–477.

43. Banan, A., S. A. McCormack, and L. R. Johnson. 1998. Polyamines are required for microtubule formation during gastric mucosal healing. *Am. J. Physiol.* 274:G879–G885.

44. Chu, P. J., H. Saito, and K. Abe. 1994. Polyamines promote neurite elongation of cultured rat hippocampal neurons. *Neurosci. Res.* 19: 155–160.

45. Chu, P. J., H. Saito, and K. Abe. 1995. Polyamines promote regeneration of injured axons of cultured rat hippocampal neurons. *Brain Res.* 673:233–241.

46. Cai, D., K. Deng, …, M. T. Filbin. 2002. Arginase I and polyamines act downstream from cyclic AMP in overcoming inhibition of axonal growth MAG and myelin in vitro. *Neuron.* 35:711–719.

47. Duan, J., and M. A. Gorovsky. 2002. Both carboxy-terminal tails of α- and β-tubulin are essential, but either one will suffice. *Curr. Biol.* 12:313–316.

48. Dent, E. W., F. Tang, and K. Kalil. 2003. Axon guidance by growth cones and branches: common cytoskeletal and signaling mechanisms. *Neuroscientist.* 9:343–353.

49. Baas, P. W., C. Vidya Nadar, and K. A. Myers. 2006. Axonal transport of microtubules: the long and short of it. *Traffic.* 7:490–498.

50. Challacombe, J. F., D. M. Snow, and P. C. Letourneau. 1997. Dynamic microtubule ends are required for growth cone turning to avoid an inhibitory guidance cue. *J. Neurosci.* 17:3085–3095.

51. Jaworski, J., L. C. Kapitein, …, C. C. Hoogenraad. 2009. Dynamic microtubules regulate dendritic spine morphology and synaptic plasticity. *Neuron.* 61:85–100.

52. Mouriño-Pérez, R. R., R. W. Roberson, and S. Bartnicki-García. 2006. Microtubule dynamics and organization during hyphal growth and branching in *Neurospora crassa*. *Fungal Genet. Biol.* 43:389–400.

53. Cason, A. L., Y. Ikeguchi, …, C. E. Schwartz. 2003. X-linked spermine synthase gene (SMS) defect: the first polyamine deficiency syndrome. *Eur. J. Hum. Genet.* 11:937–944.

54. Chen, G. G., L. M. Fiori, …, G. Turecki. 2010. Evidence of altered polyamine concentrations in cerebral cortex of suicide completers. *Neuropsychopharmacology.* 35:1477–1484.

55. Kesler, S. R., C. Schwartz, …, A. L. Reiss. 2009. The impact of spermine synthase (SMS) mutations on brain morphology. *Neurogenetics.* 10:299–305.